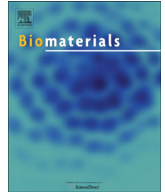




Contents lists available at ScienceDirect

Biomaterials

journal homepage: www.elsevier.com/locate/biomaterials

Long-acting beneficial effect of percutaneously intramyocardially delivered secretome of apoptotic peripheral blood cells on porcine chronic ischemic left ventricular dysfunction[☆]

Noemi Pavo^a, Matthias Zimmermann^b, Dietmar Pils^c, Michael Mildner^d, Zsolt Petrás^e, Örs Petneházy^e, János Fuzik^a, András Jakab^f, Christian Gabriel^g, Wolfgang Sipos^h, Gerald Maurer^a, Mariann Gyöngyösi^{a,1}, Hendrik Jan Ankersmit^{b,i,*,1}

^a Department of Cardiology, Medical University of Vienna, Austria

^b Department of Thoracic Surgery, Medical University of Vienna, Austria

^c Department of Obstetrics and Gynecology – Molecular Oncology Group, Medical University of Vienna, Austria

^d Department of Dermatology, Medical University of Vienna, Austria

^e Institute of Diagnostic Imaging and Radiation Oncology, University of Kaposvar, Hungary

^f Department of Biomedical Imaging and Image-guided Therapy, Medical University of Vienna, Austria

^g RedCrossTransfusion Service for Upper Austria, Linz, Austria

^h Clinical Department for Farm Animals and Herd Management, University of Veterinary Medicine, Vienna, Austria

ⁱ Christian Doppler Laboratory for Cardiac and Thoracic Diagnosis and Regeneration, Vienna, Austria

ARTICLE INFO

Article history:

Received 23 November 2013

Accepted 20 December 2013

Available online xxx

Keywords:

Cell-free regeneration therapy

Gene expression

Immunomodulation

Myocardial infarction

Remodeling

Animal model

ABSTRACT

The quantity of cells with paracrine effects for use in myocardial regeneration therapy is limited. This study investigated the effects of catheter-based endomyocardial delivery of secretome of 2.5×10^9 apoptotic peripheral blood mononuclear cells (APOSEC) on porcine chronic post-myocardial infarction (MI) left ventricular (LV) dysfunction and on gene expression. Closed-chest reperfused MI was induced in pigs by 90-min occlusion followed by reperfusion of the mid-LAD (day 0). At day 30, animals were randomized to receive porcine APOSEC ($n = 8$) or medium solution (control; $n = 8$) injected intramyocardially into the MI border zone using 3D NOGA guidance. At day 60, cardiac MRI with late enhancement and diagnostic NOGA (myocardial viability) were performed. Gene expression profiling of the infarct core, border zone, and normal myocardium was performed using microarray analysis and confirmed by quantitative real-time PCR. Injection of APOSEC significantly decreased infarct size ($p < 0.05$) and improved cardiac index and myocardial viability compared to controls. A trend towards higher LV ejection fraction was observed in APOSEC vs. controls ($45.4 \pm 5.9\%$ vs. $37.4 \pm 8.9\%$, $p = 0.052$). Transcriptome analysis revealed significant downregulation of caspase-1, tumor necrosis factor and other inflammatory genes in APOSEC-affected areas. rtPCR showed higher expression of myogenic factor Mefc2 ($p < 0.05$) and downregulated caspase genes ($p < 0.05$) in APOSEC-treated pigs. In conclusion, overexpression of MEF2c and repression of caspase was related to decreased infarct size and improved cardiac function in secretome-treated animals. Altered gene expression 1-month post-APOSEC treatment proved the long-acting effects of cell-free therapy with paracrine factors.

© 2014 The Authors. Published by Elsevier Ltd. All rights reserved.

1. Introduction

Although great effort has been made to replace infarcted myocardium with regenerative cells, the current methods have shown marginal efficacy in clinical applications [1–5]. According to the ‘dying stem cell’ hypothesis, regenerative stem cells are already undergoing apoptosis even as they are being delivered into the ischemic myocardium [4]. Thus, the best way to attenuate infarction may be to induce immunomodulatory mechanisms in a

[☆] This is an open-access article distributed under the terms of the Creative Commons Attribution License, which permits unrestricted use, distribution, and reproduction in any medium, provided the original author and source are credited.

* Corresponding author. Christian Doppler Laboratory for Cardiac and Thoracic Diagnosis and Regeneration, Department of Thoracic Surgery, Medical University of Vienna, Waehringer Guertel 43 18–20, A-1090 Vienna, Austria. Tel.: +43 1 40400 6777 (office), +43 1 40400 6857 (lab); fax: +43 1 40400 6977.

E-mail address: hendrik.ankersmit@meduniwien.ac.at (H.J. Ankersmit).

¹ H.J. Ankersmit and M. Gyöngyösi share the last authorship.

paracrine manner [5–8]. We have shown previously that the secretome of apoptotic peripheral blood cells (APOSEC), which is derived from large numbers of easily-obtainable peripheral blood mononuclear cells (PBMCs), can be used to therapeutically regenerate the myocardium after acute ischemic injury [9–12].

The optimal mode of delivering reparative cells or substances into the ischemic myocardium (i.e. intracoronary or percutaneous intramyocardial delivery) is still a matter of debate. Intracoronary delivery of cells increases the risk of temporary occlusion of the infarct-related artery and requires active migration of the cells from the vessel lumen to the injured tissue site [13]. The inherent disadvantages of cell therapy include the obvious limitations of the relatively small number of autologous adult cells that are available and the relatively large injection volume of the cells, especially for intramyocardial application [14,15]. Using APOSEC, which contains a mixture of cytokines and growth factors, might avoid the disadvantages of cell-based therapies and be more feasible while also enhancing therapeutic efficiency.

Due to the early death of many regenerative cells when injected into the necrotic core, intramyocardial regenerative therapies instead target the infarct border zone, which shows signs of hibernating myocardium. Interestingly, some reports have described the metabolic, proteomic, and genomic differences between the infarct core and remote (normal) myocardium, but there is no genomic information about this special border zone of infarction

[16,17]. Furthermore, no studies have investigated the effects of secretome-based therapies on gene expression in the core and border zone of myocardial infarction (MI).

We hypothesized that percutaneous intramyocardial delivery of APOSEC would be safe and effective in a clinically relevant porcine model of chronic left ventricular (LV) dysfunction after MI. We further hypothesized that the trophic effect of APOSEC could cause structural changes, leading to improved hemodynamic function post-MI via altered gene expression. In our experiments we have injected APOSEC or placebo locally intramyocardially into the border zone of infarction using the catheter-based 3D NOGA-guided intramyocardial application method and investigated the LV function, infarct size and gene expression of the ischemic injured myocardium.

2. Materials and methods

2.1. Porcine model of acute MI and APOSEC production

This study used a porcine closed-chest reperfused acute MI model. Domestic pigs ($n = 22$) underwent percutaneous 90-min balloon occlusion of the mid-left anterior descending coronary artery (LAD) followed by reperfusion (Fig. 1 and Supplementary Materials and Methods). APOSEC was produced from pig PBMCs (Supplementary Materials and Methods). Animal investigations were carried out in accordance with the “Position of the American Heart Association on Research Animal Use,” as adopted by the AHA on November 11, 1984. The study was approved by the Ethics Committee on Animal Experimentation at the University of Kaposvar, Hungary.

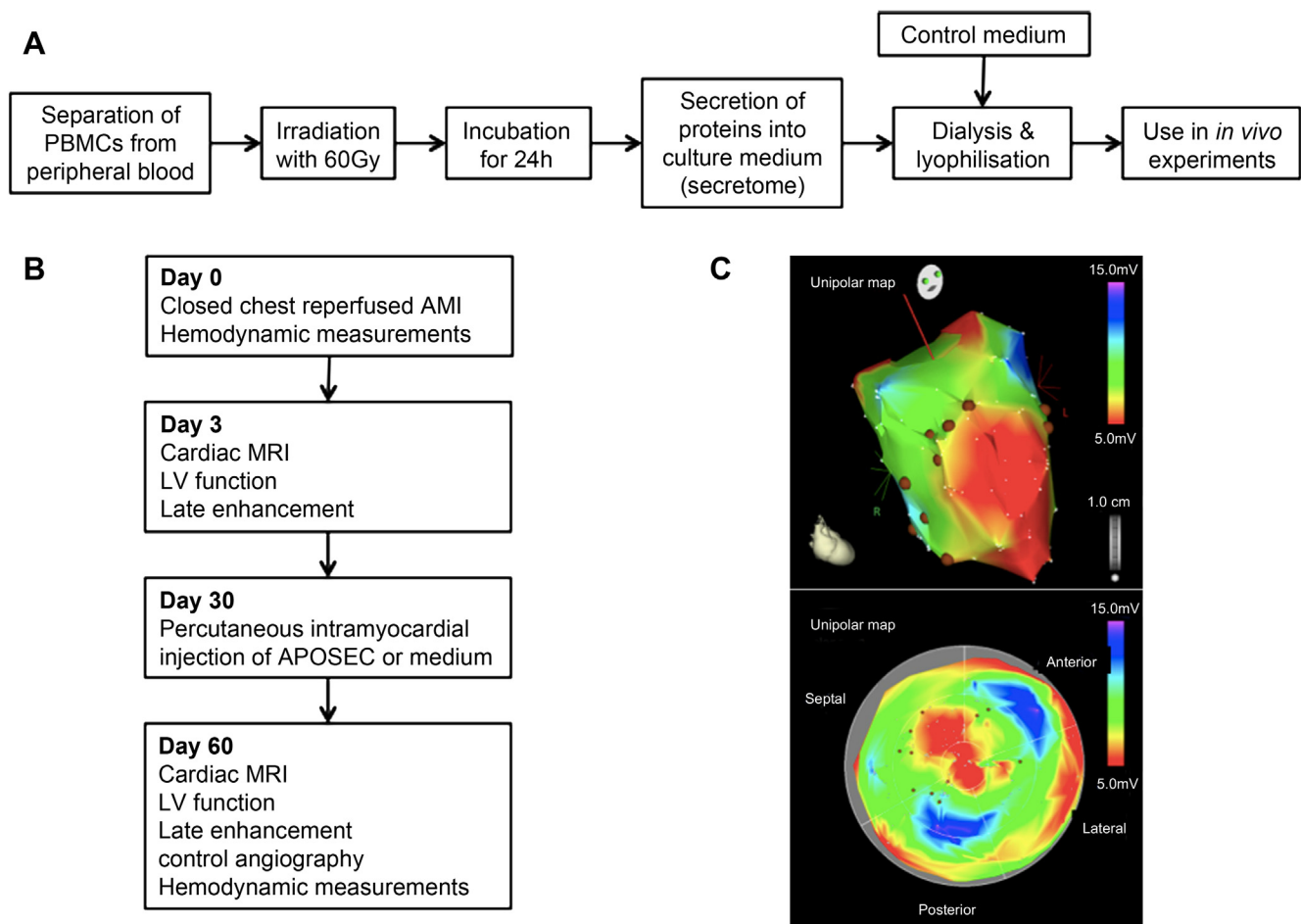


Fig. 1. Study design. A. Schematic showing how APOSEC is prepared from peripheral blood mononuclear cells (PBMCs). B. Study design. C. 3D views of the left ventricle derived by NOGA endocardial mapping and NOGA-guided injection into the border zone of chronic infarction. Brown dots mark the locations of the intramyocardial injections in the border zone of infarction. Color-coded 3D image (upper) were converted to a 2D polar map (below). Red represents non-viable infarcted myocardium, while green and yellow indicated the border zone of infarction. Normal viable myocardium is colored blue and purple.

2.2. Percutaneous intramyocardial delivery of APOSEC or medium solution using 3D NOGA guidance

One month after MI (day 30; development of scar and LV remodeling; Fig. 1), the animals were sedated, intubated, and the patency of the infarct-related artery was confirmed by coronary angiography. LV hemodynamic parameters were measured via pigtail catheters. NOGA endocardial mapping was performed using a percutaneous NOGA Star catheter (Cordis, Johnson & Johnson, Miami Lakes, FL, USA) as described previously [18]. After creation of the 3D shape of the LV infarction, the diagnostic NOGA Star catheter was replaced by a NOGA MyoStar injection catheter (Cordis, Johnson & Johnson). The pigs were randomized to receive either APOSEC (derived from 2.5×10^9 PBMCs, resuspended in 4 ml physiologic saline, 300- μ l aliquots) or medium as a control (resuspended lyophilized Cell Growth medium) in 11 ± 1 locations of the border zone of infarction using 3D NOGA-guided percutaneous intramyocardial delivery. The animals were allowed to recover. At 60 days post-infarction (30 days post-injection), control coronary angiography and NOGA endocardial mapping were performed while the pigs were under general anesthesia.

2.3. Cardiac magnetic resonance imaging (MRI)

Cardiac MRI with late enhancement (LE) was performed 3 days and 60 days after the reperused acute MI procedure using a 1.5-T clinical scanner (Avanto, Siemens, Erlangen, Germany) with a phased-array coil and a vector ECG system (Supplementary Materials and Methods). The LV end-diastolic (EDV) and end-systolic (ESV) volumes, ejection fraction (EF), and infarct size were measured (Supplemental Materials and Methods) [19].

2.4. LV hemodynamic measurements

LV hemodynamic measurements were performed via pigtail catheter and included systolic aortic pressure, LV systolic and end-diastolic pressures (EDP), LV contractility expressed as dp/dt and $dp/dt/P$, and LV end-diastolic stiffness (LV EDP/EDV).

2.5. Myocardial viability, infarct transmural and regional functional assessment by NOGA

Using the 12-segment polar map analysis principles, the mean unipolar, bipolar, and local linear shortening values (UPV, BiP, and LLS, respectively) of the injected areas were calculated and reported as mV or %, respectively.

2.6. Histology

The hearts were explanted at day 60 and sliced, and representative specimens of normal tissue and of the border zone and infarcted areas were fixed in 10% neutral buffered formalin, embedded in paraffin, sectioned, and stained for hematoxylin-eosin, angiogenic marker of CD31 and stem cell factor CD117 (Supplemental Materials and Methods).

2.7. Gene expression analysis using RNA microarrays and real-time PCR (rtPCR)

Tissue samples for RNA extraction were obtained directly from the infarct core, border zone, and remote myocardium and stored in RNAlater (Qiagen, Germany) at -20°C . Total RNA was isolated from tissue samples using the RNeasy Microarray Tissue Mini Kit (Qiagen, Germany). RNA quality was checked on RNA Nano chips using the Agilent 2100 Bioanalyzer platform (Agilent Technologies).

2.7.1. RNA microarrays

Microarray gene analysis was performed by Miltenyi (Miltenyi Biotec GmbH, Germany) (Supplementary Materials and Methods). The fluorescence signals of the hybridized Agilent Microarrays were measured using Agilent's Microarray Scanner System (Agilent Technologies) and analyzed using Agilent Feature Extraction Software (FES).

Raw hybridization values were loaded into R (GNU R) using the R-package limma (v3.14.4) [20,21]. Microarray data have been uploaded to the Gene Expression Omnibus database (<http://www.ncbi.nlm.nih.gov/geo/query/acc.cgi?acc=GSE47397>). Biological interpretation of significant gene lists was performed using the Database for Annotation, Visualization and Integrated Discovery (DAVID) v6 [22]. Data were reported in annotational clusters or as single gene expression, heat maps, and Venn diagrams.

2.7.2. rtPCR of selected genes

The mRNA of myocardial probes of all 3 regions from both groups of pigs was reverse transcribed to cDNA (Qiagen, Germany) and expression was quantified by rtPCR (Applied Biosystems 7500 Real-Time PCR System, Life Technologies, USA). The primers for the target sequences were designed using Primer3 software (http://primer3.wi.mit.edu/primer3web_help.htm; Microsynth, Switzerland) (Supplemental Table 1). The expression rates of the target genes were normalized to the geometric means of the housekeeping genes GAPDH, HPRT1, and PPIA, which were selected as endogenous controls due to their stable expression. The relative gene expression level was calculated using the ΔCt method (i.e. expression level

relative to an endogenous control). The expression changes were calculated relative to expression levels in the normal myocardium of the same animal.

2.8. Statistics

Continuous data of the two groups of pigs are reported as mean \pm standard deviation. Differences between the groups were tested using the Student's *t* test for continuous variables and the χ^2 test for categorical variables. A difference was considered statistically significant at $p < 0.05$. Data analyses and interpretations were performed by an experienced observer who was blinded to the randomization and to all study results. Statistical analysis was performed using SPSS 18.0 (SPSS Inc, USA) software.

For gene array analysis, to test for all comparisons (i.e. differences between regions of interest: normal, border, and infarct and APOSEC vs. control) a linear model for each gene was fitted and the estimated coefficients and standard errors for these contrasts were computed. Subsequently, moderated *t*-statistics, moderated *F*-statistics, and the log-odds of differential expression were calculated by empirical Bayes shrinkage of the standard errors towards a common value. False discovery rates (FDR) below 5% were considered statistically significant for each comparison. Higher FDR cut-offs were used for some contrasts, especially for the use of the gene lists for biological interpretation. Unsupervised hierarchical clustering was performed with the Euclidean distance as the distance function and the Ward algorithm in R, using centered and scaled log₂ expression values. Principal Component Analysis (PCA) was also performed for centered and scaled values.

3. Results

3.1. Effect of APOSEC on infarct size and hemodynamics

Six pigs died during the reperused MI procedure ($n = 5$) or 2 days later ($n = 1$). The remaining 16 pigs were randomized to the APOSEC group ($n = 8$) or to the control group ($n = 8$).

Figs. 2 and 3 show the 3-day and final MRI data. Compared to control animals, the APOSEC-treated animals had significantly smaller infarcts ($13.92 \pm 1.34\%$ vs. $21.58 \pm 2.09\%$, $p < 0.05$) and a significantly higher cardiac index (4.40 ± 3.94 l/min/m² vs. 3.07 ± 2.35 l/min/m², $p < 0.05$). There was also a trend towards a higher EF ($45.4 \pm 5.9\%$ vs. $37.4 \pm 8.0\%$, $p = 0.052$) and significant changes in LV EF from baseline to follow-up (FUP) in the APOSEC-treated vs. control animals. The area at risk as measured by MRI at day 3 was similar in the two groups ($46 \pm 9\%$ vs. $45 \pm 10\%$ of the entire LV myocardium).

The baseline, pre-injection, and post-injection hemodynamic data was not different between the groups (data not shown). Significantly lower EDP and end-diastolic stiffness was measured in the APOSEC group at the final FUP (Fig. 3). Infarct transmural, as assessed by MRI and NOGA bipolar maps, showed smaller transmural infarctions in the APOSEC-treated pigs (Fig. 2). The APOSEC-treated animals had significantly higher UPV and BiP values for the treated area with a trend towards higher LLS (Fig. 4).

3.2. Angiogenesis and homing of endogenous c-kit positive cells in the border zone of experimental MI

There was a significant increase in the number of CD31+ cells in the APOSEC group in the border zone of infarction, indicating enhanced angiogenesis (Fig. 5). The CD31+ cell density per DAPI positive cells in the infarct and border zone were $15.3 \pm 1.9\%$ vs. $12.6 \pm 4.5\%$ and $19.9 \pm 1.8\%$ vs. $11.3 \pm 3.2\%$ in the APOSEC vs. controls. Significantly ($p < 0.05$) higher numbers of CD117+ cells were found in infarct core ($2.0 \pm 0.9\%$ vs. $0.6 \pm 0.7\%$) and border area ($3.0 \pm 1.4\%$ vs. $0.9 \pm 0.8\%$) in APOSEC-pigs suggesting enhanced accumulation of endogenous cardiac stem cells as compared with medium-treated animals.

3.3. Gene expression differences between APOSEC- and medium-treated animals

Differential gene expression of infarcted, border zone, and remote myocardium in the chronic failing hearts before treatment is

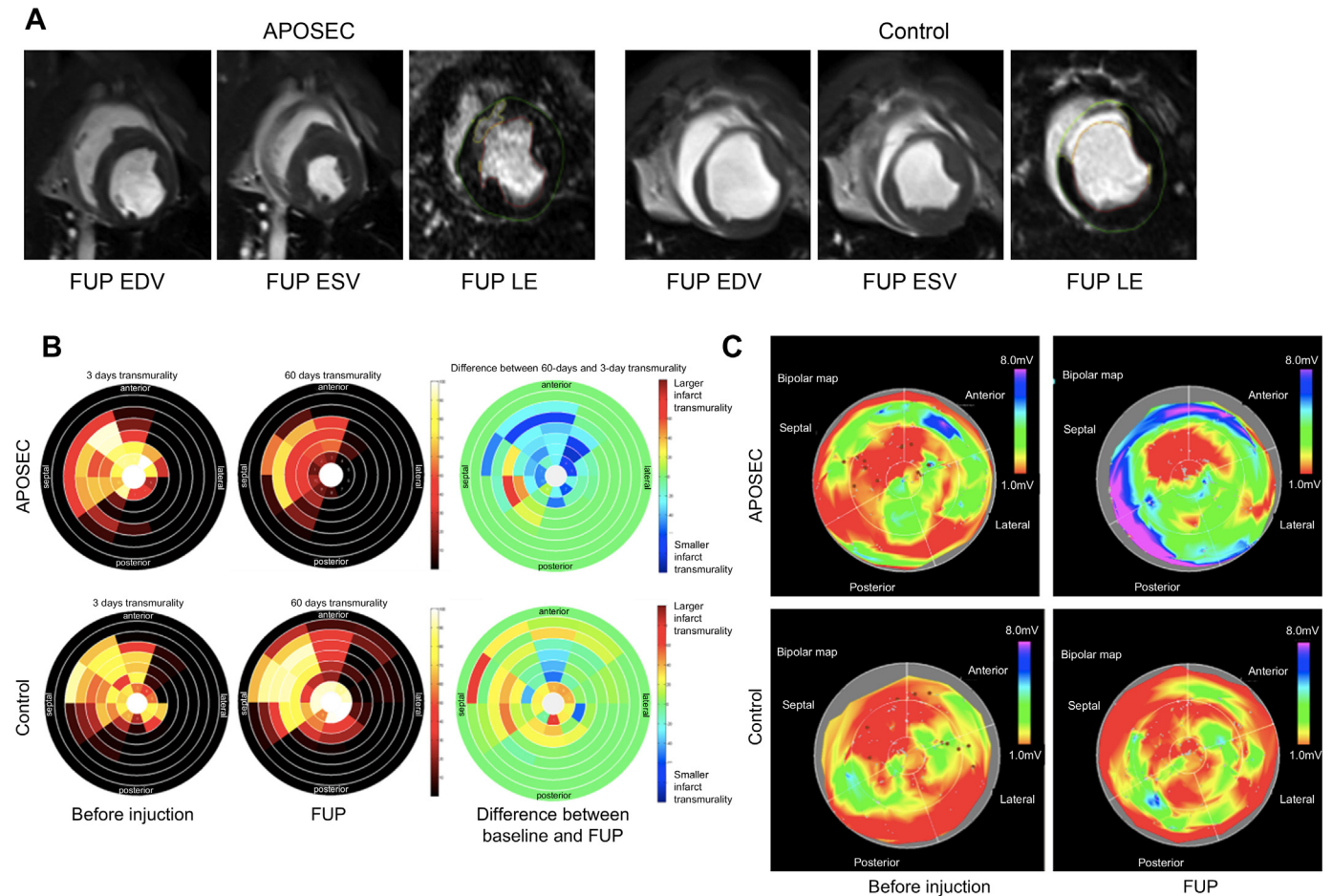


Fig. 2. Left ventricular function and infarct transmuralty assessed by MRI and NOGA. **A.** Short axis views of follow-up (FUP) late enhancement (LE) magnetic resonance images show end-diastolic (EDV) and end-systolic (ESV) contours with LE 30 days after percutaneous intramyocardial injection of APOSEC or medium solution. Note the reduced ventricular volumes and infarct area in an APOSEC-treated pig. **B.** Bull's eye plots of LE-MRI data demonstrating treatment effects in representative APOSEC-treated (top row) and medium-treated (control) pigs (bottom row). Note that segmental infarct transmuralty is reduced in the FUP images of an APOSEC-treated pig, while slight enlargement of the infarct area is seen in a medium solution-treated pig. The following segments are affected: middle anterior, middle anteroseptal, apical anterior, and apical septal. Left and middle panels: segmental infarct transmuralty in 3-day and 30 days after injection (FUP, day-60) MR images. Transmuralty was measured as the percentage of the LE area (i.e. the scar) relative to the volume of the corresponding myocardial segment. Right panels: treatment effects as visualized by differences between FUP and day-3 segmental measurements. Positive values refer to growing segmental infarct transmuralty (red) while negative values indicate reduced infarct transmuralty (blue). **C.** Bull's eye plots of NOGA bipolar (transmuralty) maps at baseline (injection) and FUP corresponding to the MRI polar plots (B) in the same APOSEC- and control pigs. Red represents greater infarct transmuralty.

shown in the [Supplemental Results](#). PCA and hierarchical clustering of the gene expression patterns of the corresponding myocardial areas in APOSEC- and medium-treated animals revealed 10 genes in the infarct core and 23 genes in the globally treated areas (infarct core and border zone) that showed significantly different expression compared to remote myocardium ([Fig. 6](#), [Table 1](#)). Systematic and integrative gene analysis using DAVID Bioinformatics Resources identified and classified only a portion of the significantly up and downregulated genes (11 of 23 genes, 47.8%). Due to the expression of single genes in several pathways, these genes could not be classified into unique clusters. There was significant downregulation of apoptosis-, inflammation-, and lipid metabolism-associated genes. This included repression of caspase-1 (apoptosis-related cysteine peptidase and interleukin 1-beta-convertase), tumor necrosis factor alpha (TNF-alpha), stromal derived factor (SDF)2-like protein 1 (endoplasmic reticulum stress-inducible gene), arachidonate 15-lipoxygenase (lipid metabolism), uroplakin 1B (coding a transmembrane protein), claudin 3 (tight junction protein), and other genes that were not characterized further.

Using less-stringent criteria (FDR <10%), additional 53 genes were detected that showed different expression levels in the APOSEC group vs. the control group. Of these, 24 genes were

identified by the functional annotation analysis ([Table 1](#)). Six of the 24 genes were overexpressed, while 18 were repressed.

The APOSEC-affected myocardial area showed upregulation of insulin-like growth factor (an angiogenic growth factor), Kruppel-like factor (a regulator of vascular tone and homeostasis and an anti-atherogenic), myozenin (a gamma-filamin and alpha-actinin-binding protein in skeletal muscles), and a gene similar to glyceronephosphate O-acyltransferase (thought to protect cells from oxidative stress). In contrast, some of the downregulated genes belonged to the inflammatory and immune system superfamily: killer cell lectin-like receptor subfamily K, cystatin F, ectonucleoside triphosphate diphosphohydrolase 1, CD2, complement component 1 q subcomponent, A-chain, C-X-C motif ligand 9 and 10, C-type lectin domain family 5, member A, CD247, and beta-2 microglobulin. Other downregulated genes included some involved in lipid metabolism (a scavenger receptor for phosphatidylserine and oxidized low density lipoprotein), a histocompatibility antigen (MHC class II DR-alpha), a structural matrix protein (ameloblastin), and other less well characterized genes (suppression-inducing transmembrane adapter 1).

If FDR <20% was used (data available at the GEO homepage), additional annotated overexpressed genes in the border area of

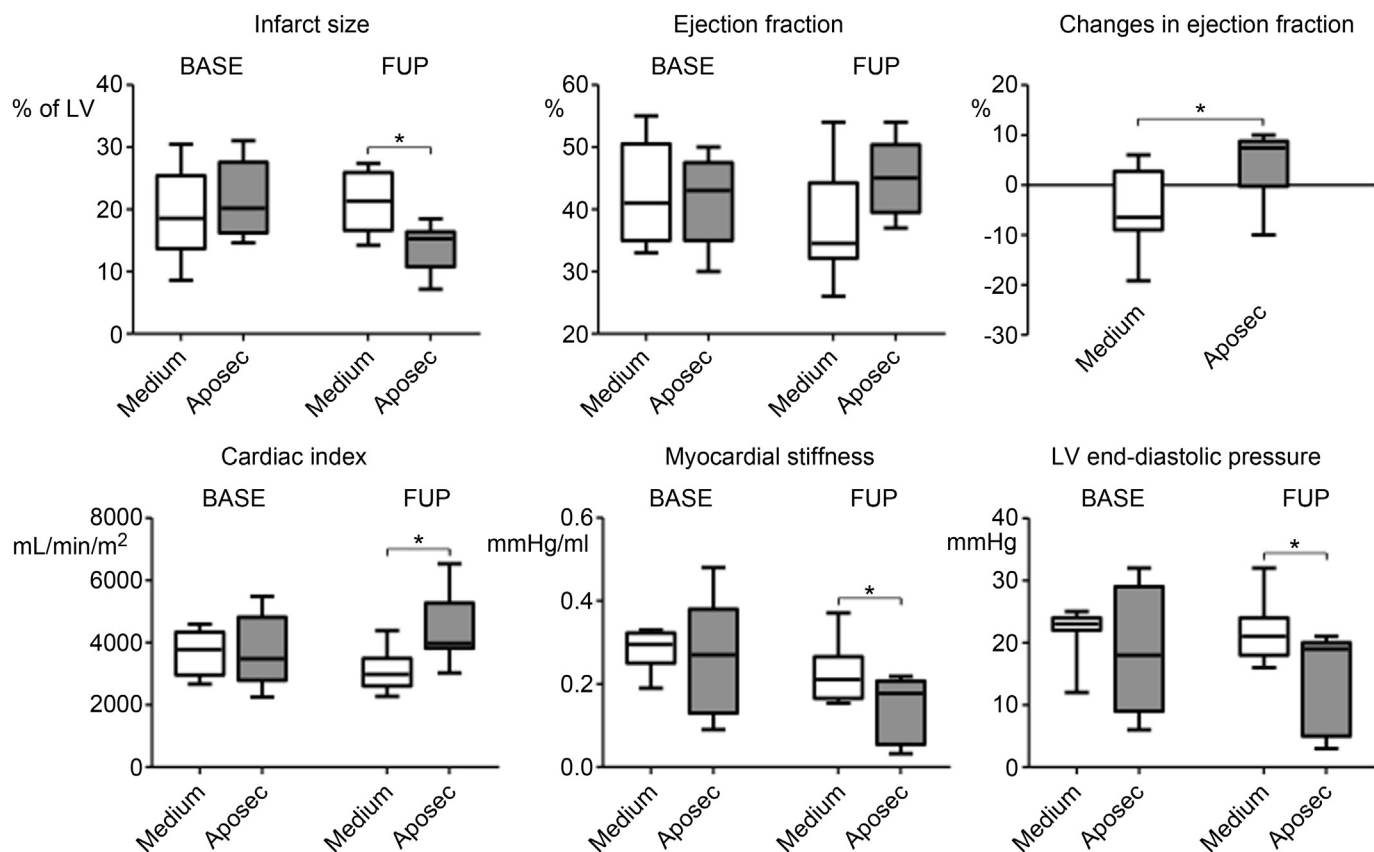


Fig. 3. MRI results. Ejection fraction (EF) at day 3 (BASE) and at day 60 (follow-up; FUP) showing a significant increase in EF at FUP in the APOSEC-treated pigs ($n = 8$) compared to the control pigs ($n = 8$). The APOSEC-treated pigs showed significantly smaller infarct size and better cardiac indexes. There was significantly lower end-diastolic pressure and end-diastolic stiffness in the APOSEC-treated group. * $p < 0.05$.

APOSEC-treated animals belonged to 42 clusters (an additional 686 genes). These clusters included genes involved in purine metabolism (phosphodiesterase 3A, 4A, and 4B, pyruvate kinase), in the cell cycle (e.g. fuzzy/cell division cycle 20 related 1), in the calcium signaling pathway (adrenergic beta-1 receptor, nitric oxide synthase 2, inducible, calmodulin), and in regulation of the actin cytoskeleton (fibronectin receptor, vinculin/cell adhesion related gene/). The clusters also included other cardiac-related genes, such as myocardin (important for cardiomyocyte survival and maintenance), GATA-binding protein 4 (transcription factor needed for normal heart development), and adrenergic beta-1 receptor. The main clusters of downregulated genes in the border zone of the APOSEC-treated animals included genes responsible for toll-like receptor pathways (CD40 molecule, CD86 molecule, chemokine ligands, interleukin-1 receptor-associated kinase 4, and toll-like receptor 3 and 7, which are responsible for the innate immune response and mediation of ischemic/reperfusion injury), and genes involved in cardiomyopathy (transforming growth factor beta).

3.4. rtPCR

rtPCR analysis of mRNA expression in the border zone of infarction in the APOSEC-treated animals confirmed that there was significant overexpression of the cardiac myogenesis and vascular development gene, myocyte-specific enhancer factor 2C (MEF2c), and repression of the apoptosis regulator caspase-3 (Fig. 6). In the border zone, there was a trend towards higher expression ($p < 0.1$) of angiogenic regulatory factor hypoxia-inducible factor 1-alpha and transcription factor GATA-4 in the APOSEC group compared

with the control group. There were no significant differences between the groups in terms of the expressions of genes involved in stem cell homing (CXCR12), the transcription factor myogenin, and the extracellular matrix metalloproteinase-9 and transforming growth factor beta.

4. Discussion

Here we demonstrated that 3D NOGA-guided injection of APOSEC is safe, feasible, and effective. APOSEC injection was associated with an enhanced vascular density and homing of c-kit+ endogenous stem cells in the peri-infarct and infarcted area, with a reduction of infarct size, and with a significant increase in LV EF contractile function. Gene profiling analysis of the APOSEC-treated myocardial areas revealed that there was downregulation of inflammatory and apoptotic genes. Post-hoc validation of gene expression by rtPCR showed higher expression levels of myogenic factor and *Mefc2* and robust downregulation of apoptosis regulator caspase-3.

We previously showed that similar to the secretome of mesenchymal stem cells (MSCs) [23], APOSEC contains anti-apoptotic and regenerative factors that promote angiogenesis and myocardial repair [11,12]. In contrast to MSCs, PBMCs contain different types of mononuclear cells. However, one big advantage of PBMCs is that the available autologous cells are numerous. Even if ex vivo cell culture expansion of MSCs might provide sufficient quantities of secretome, the biological characteristics of the MSC secretome depend on the number of passage of the cells with possibility to chromosome variability after passage 4, and on the cell donor, making it difficult to standardize secretome production

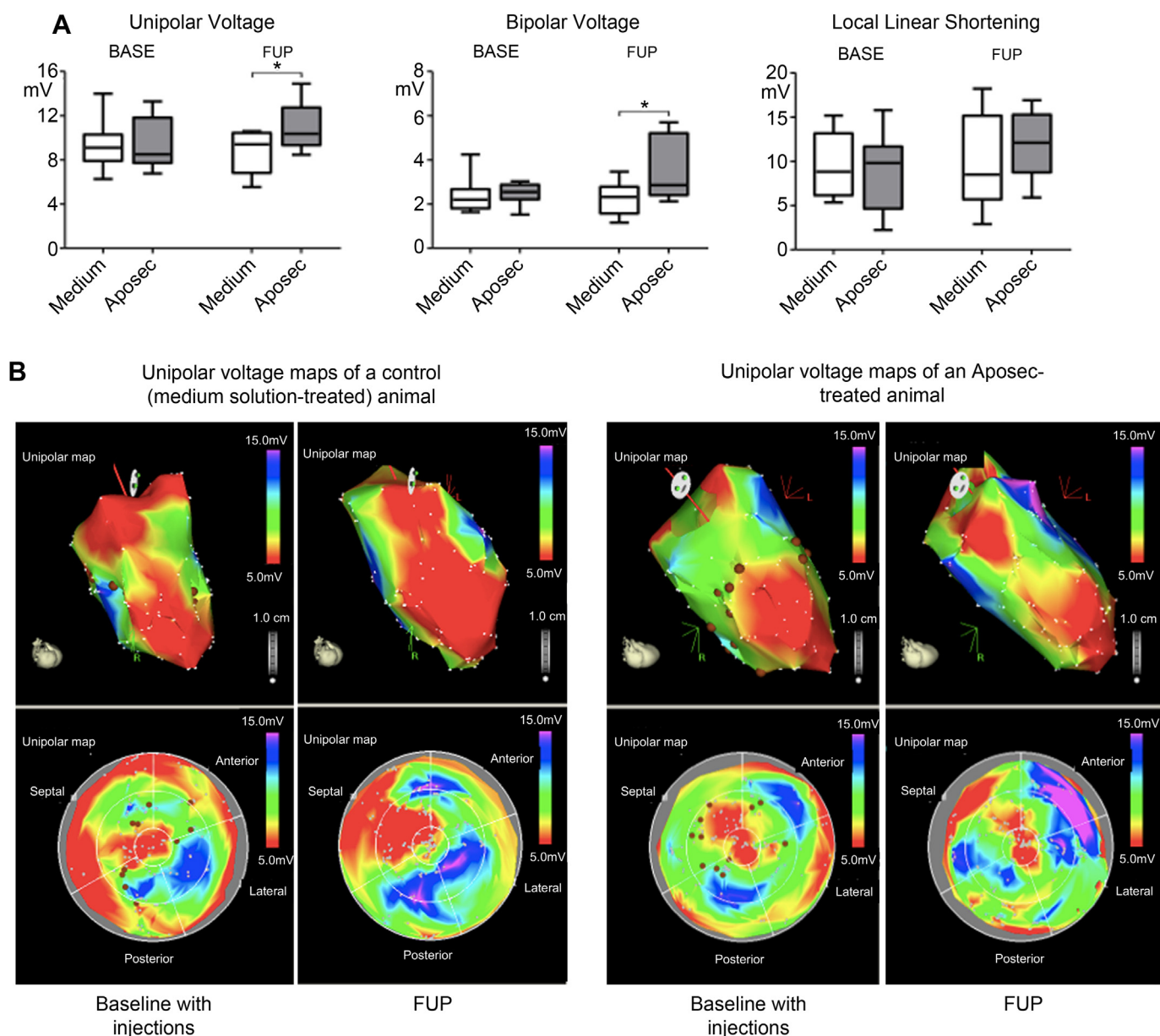


Fig. 4. NOGA results and representative NOGA images. A. Baseline (BASE) and follow-up (FUP) unipolar voltage (an index of myocardial viability) of the injected area of APOSEC- and medium-treated (control) pigs. At FUP (day-60), the APOSEC group had significantly higher unipolar voltage values (left) and bipolar voltage (index of infarct transmuralty) values. There were trends towards higher local linear shortening voltage values (an index of segmental wall motion) at FUP. B. Representative NOGA images show the injection points around the infarcted area in APOSEC- and medium-treated pigs. The infarcted area is visibly smaller at FUP in the APOSEC-pigs, indicating that ventricular remodeling was reduced in these animals. Color coding is as defined in Fig. 1.

in large amount. Notably, a pre-defined mixture of known regenerative factors did not exert effects that were similar to those of the naturally derived secretome [23].

Our experiments investigated changes in the gene expression profile of the host tissue (ischemically injured myocardial cells) after direct contact with the injected mixture of paracrine factors (APOSEC). Even if reparative cells in cell-based therapies that are delivered to the ischemic area produce numerous signaling molecules, such as matrix proteins and anti-inflammatory and angiogenic substances, the host tissue response is the crucial factor in myocardial tissue regeneration.

Changes in gene expression in ischemic cells depend on the severity of the injury. Interestingly, APOSEC mainly caused gene silencing in the pro-inflammatory cascade along with, to a lesser extent, some gene induction. However, it is important to note that

almost half of the downregulated genes, and none of the upregulated genes, had currently known functions. These latter genes might belong to metabolic, angiogenic, or myogenic functional clusters that cause synergistic regenerative processes as demonstrated by infarct size reduction and prevention of ventricular remodeling.

4.1. APOSEC induces long-lasting differences in gene expression

Although the studies were exploratory, previous analyses of the gene expression profiles of chronically infarcted, reperfused, and remodeled ischemic myocardium identified functional uni- or bimodal genes with known functions [24–30]. The published data, which are mostly from studies conducted in rodent MI models, are heterogeneous in terms of the number and type of differentially-

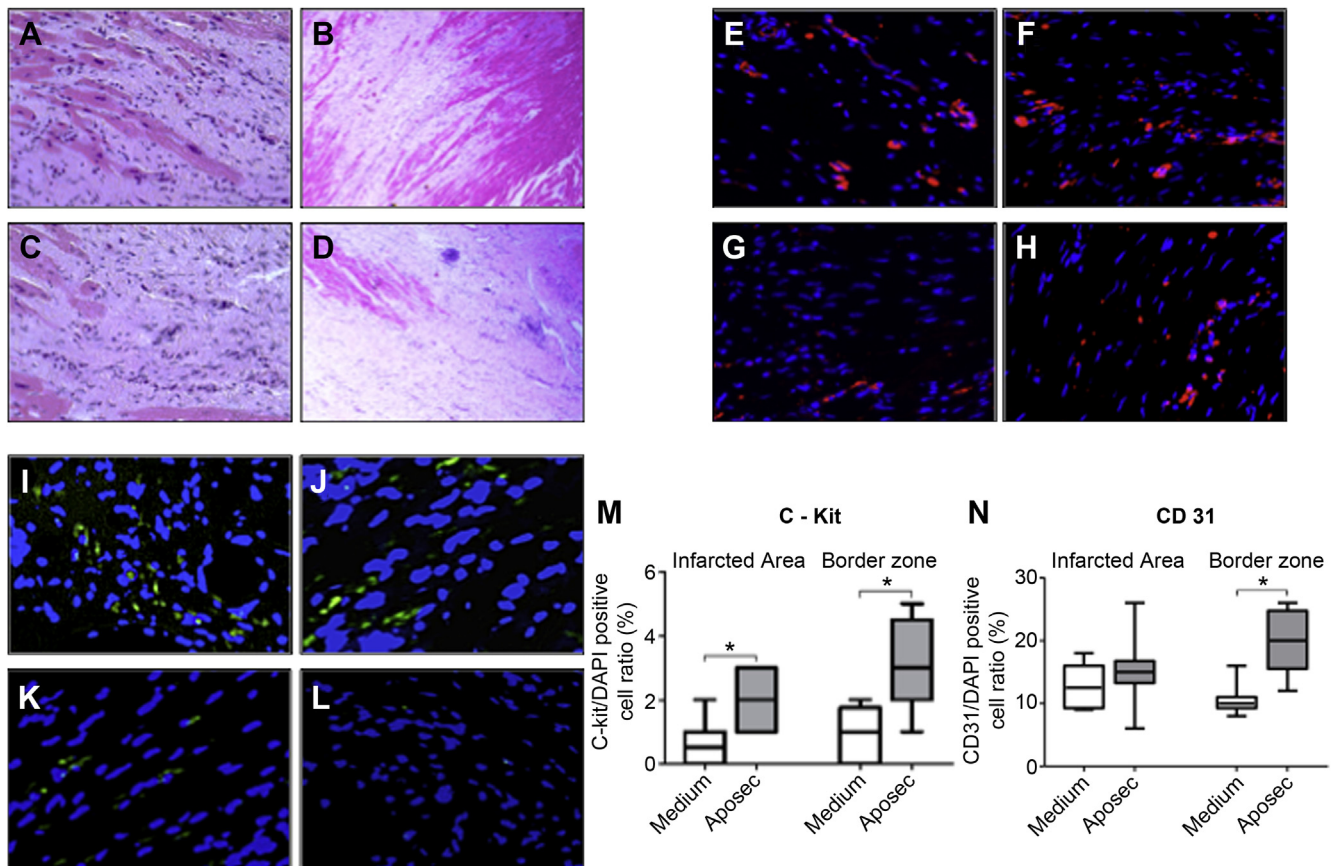


Fig. 5. Angiogenic effect of APOSEC. A–D. H&E stained porcine myocardium 60 days after induction of myocardial infarction and treated with intramyocardial injection of APOSEC or medium (infarct core A and C, /40 \times magnification/, and border zone of infarction B and D, /10 \times magnification/, respectively). E–H. Immunofluorescence CD31+ staining of the infarct core (E and G) and border areas (F and H) of an APOSEC or medium-treated pig, respectively. Red indicates CD31+ cells, counterstaining with DAPI. I–L. CD117 (c-kit+) immunofluorescence staining of the infarct core (I and K) and border areas (J and L) of an APOSEC or medium-treated pig, respectively. Green color represents CD117+ cells, counterstained with DAPI. M and N. APOSEC-treated pigs show a higher density of CD31+ and CD117+ cells both in infarct core and border areas, indicating enhanced level of microvascularization and homing of endogenous c-kit+ cardiac stem cells ($*p < 0.05$).

expressed genes. To our knowledge, this is the first report on gene expression profiles in closed-chest reperfused MI and also the first report to describe molecular biological changes in remote and infarcted myocardium and in the border zone of infarction (Supplemental Discussion).

Locally injected APOSEC contains paracrine factors proven to be anti-inflammatory, leading to repression of active pro-inflammatory genes, such as genes coding for TNF-alpha, SDF2-like protein 1, and caspase-1. However, several genes that showed significantly changed expression are currently not assigned to known function. The expansion of the FDR <5% cut-off to a FDR <10% cut-off gave more information about changes in gene expression in APOSEC-treated areas. Specifically, this less-stringent cut-off identified several relevant genes with altered expression. There was upregulation of angiogenic factors and other vascular tone and homeostasis regulators and repression of pro-inflammatory genes such as complement components and histocompatibility antigens.

4.2. Comparison with literature data

In contrast to the large animal model of reperfused MI used here, Jameel et al. surgically ligated the first and second diagonal branches of LAD of mini-swine and immediately injected 50 million bone marrow-derived multipotent progenitor cells [31]. This surgical cell transplantation resulted in a marked improvement in EF (51.2% vs. 35.7%) and in a decrease in infarct size (4.6% vs. 8.6%) at the 4-month FUP in treated vs. control groups, respectively,

without engraftment of the cells. Gene expression analysis revealed 41 downregulated and 11 upregulated genes in the cell transplantation group; the authors attributed these changes to the paracrine effects of the injected cells. There was also downregulation of genes in the inflammatory pathway, similar to what was seen in our experiments. The differences between the gene expression pathways identified in the two studies may due to the use of different MI models and treatments as well as to the presence of different paracrine mediators.

Similar to the MSC secretome [23], the secretome of apoptotic PBMCs (i.e. APOSEC) has the potential to block apoptosis and local inflammation, enhancing neoangiogenesis and limiting infarct expansion and remodeling. Through overexpression of regulatory genes at the FDR <10% level, such as Kruppel-like factor and myozenin, it is possible that APOSEC acts to restore vascular and muscle homeostasis. We did not see changes in any genes that are known to contribute to endogenous regeneration via the mobilization and homing of cardiac or bone marrow stem cells, such as genes coding for SDF-1 or for chemotactic cytokines. There is also the question of the importance of isolated gene expression i.e. expression of genes that are not functionally related to each other or that are in different pathways. However, small changes in the function of a key gene can act as a signal that triggers a biologically relevant effect.

rtPCR of selected genes confirmed the significant repression of the apoptosis regulator caspase-3. The increase in expression of hypoxia-inducible factor 1-alpha and GATA-4 in the border zone of

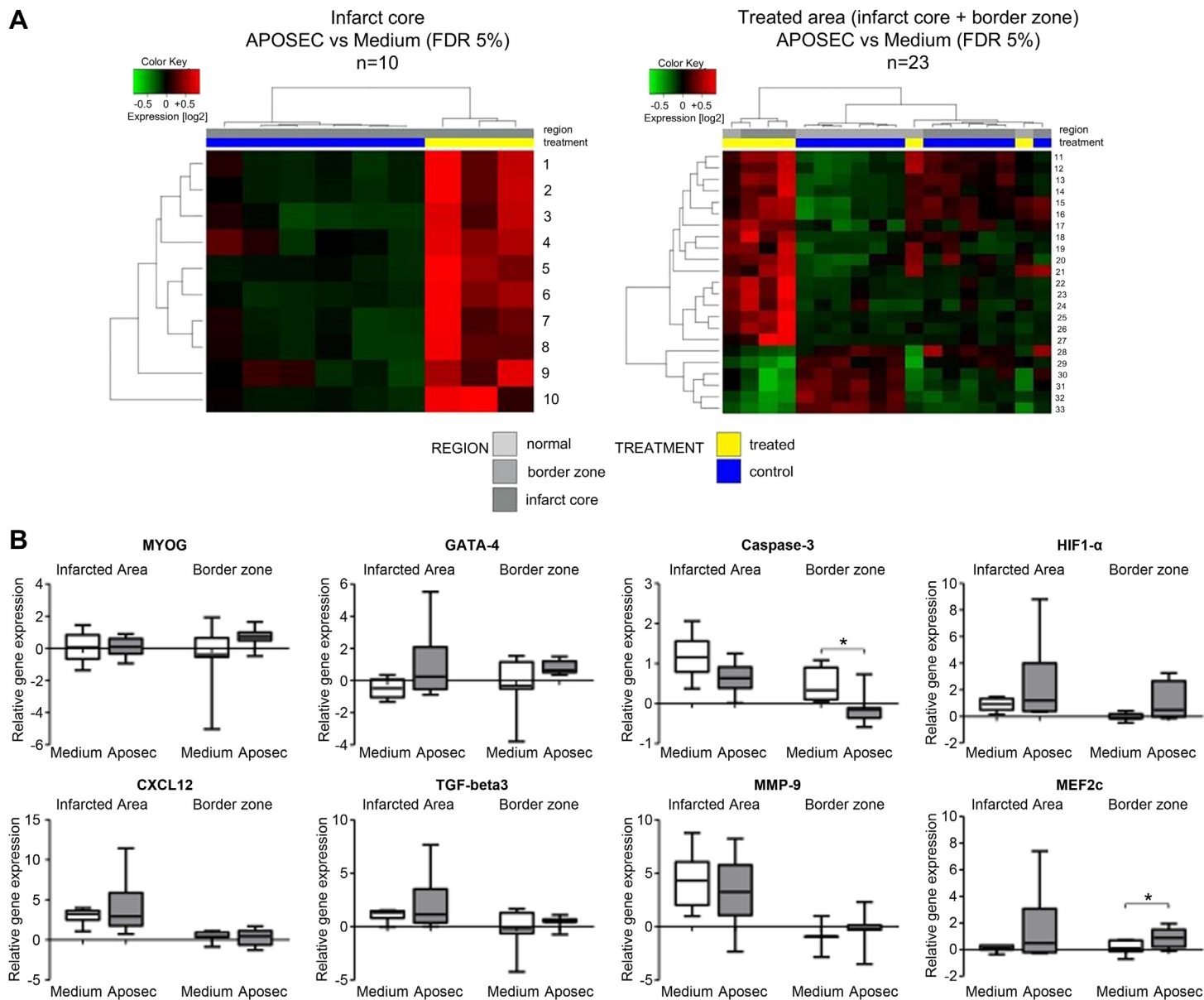


Fig. 6. Gene array analysis of differential expression of gene clusters in APOSEC-treated and medium-treated pigs in the infarct core and treated region (infarct core and border zone). A. Comparison of genes with significantly different expression levels [false discovery rate (FDR) 5%] in infarct (left) and treated regions (right; infarct core and border zone) of APOSEC- and medium-treated pigs (clustered and reported as a heat map). Name of genes: 1 = similar to LOC513955 protein; 2 = CD209 molecule; 3 = n.i.; 4 = claudin 3; 5 = n.i.; 6 = similar to trichohyalin; 7 = arachidonate 15-lipoxygenase; 8 = epididymal secretory protein; 9 = CD209 molecule; 10 = uroplakin 1B; 11 = n.i.; 12 = n.i.; 13 = n.i.; 14 = similar to trichohyalin; 15 = similar to Uncharacterized protein CXorf21 homolog; 16 = n.i.; 17 = caspase 1, apoptosis-related cysteine peptidase (interleukin 1. beta. convertase); 18 = n.i.; 19 = n.i.; 20 = tumor necrosis factor (ligand) superfamily member 13b; 21 = similar to Stromal cell-derived factor 2-like protein 1 precursor (SDF2-like protein 1) (PWP1-interacting protein 8); 22 = similar to LOC513955 protein; 23 = arachidonate 15-lipoxygenase; 24 = n.i.; 25 = epididymal secretory protein; 26 = uroplakin 1B; 27 = n.i.; 28 = n.i.; 29 = n.i.; 30 = n.i.; 31 = claudin 3; 32 = similar to Protein S100-A2 (S100 calcium-binding protein A2) (Protein S-100L); 33 = n.i. n.i. = not identified genes. B. Results of real-time PCR analysis of the expression of selected genes in APOSEC- and medium-treated pigs: HIF1- α : hypoxia-inducible factor 1- α ; MMP-9: matrix metalloproteinase-9, CXCL12: chemokine (C_X_C motif) ligand-12; MEF2c: myocyte-specific enhancer factor 2c; MYOG: myogenin; GATA-4: zinc finger transcription factor that binds to the DNA sequence "GATA"-4; TGF- β 3: transforming growth factor- β 3. Y axis: expression level normalized to gene expression of the normal myocardium. Each group: $n = 8$. * $p < 0.05$.

Table 1

Up and downregulated genes of the infarct core and combined treated (infarct core and border zone) areas in the APOSEC-treated animals.

Systematic name	Log fold changes	Adjusted P value	Name of gene	Regulation in APOSEC group
Infarct core FDR5%				
NM_001129972	-1.426	0.029	CD209 molecule	Down
NM_213931	-3.367	0.038	Arachidonate 15-lipoxygenase	Down
ENSSSCT00000010283	-0.675	<0.001	Similar to LOC513955 protein	Down
NM_001160075	-0.798	<0.001	Claudin 3	Down
ENSSSCT00000013027	-2.047	0.005	n.i.	Down
NM_001123212	-1.081	0.001	Uroplakin 1B	Down
TC533994	-1.573	0.043	n.i.	Down
ENSSSCT00000008105	-1.249	0.016	Epididymal secretory protein	Down
XM_001927650	-0.847	0.002	Similar to trichohyalin	Down
Combined treated areas FDR5%				
NM_214162	-1.887	0.029	Caspase 1-apoptosis-related cysteine peptidase (interleukin 1-beta-convertase)	Down
NM_001097498	-0.753	0.015	Tumor necrosis factor (ligand) superfamily member 13b	Down
ENSSSCT00000010283	-0.815	0.003	Similar to LOC513955 protein	Down
NM_001160075	-0.949	0.005	Claudin 3	Down
ENSSSCT00000013346	-1.18	0.007	Similar to uncharacterized protein CXorf21 homolog	Down
NM_001123212	-1.287	0.01	Uroplakin 1B	Down
ENSSSCT00000011046	-1.623	0.014	Similar to stromal cell-derived factor 2-like protein 1 precursor (SDF2-like protein 1) (PWP1-interacting protein 8)	Down
ENSSSCT00000007208	-2.936	0.015	Similar to Protein S100-A2 (S100 calcium-binding protein A2) (Protein S-100L)	Down
ENSSSCT00000008105	-1.249	0.016	Epididymal secretory protein	Down
XM_001927650	-0.908	0.022	Similar to trichohyalin	Down
NM_213931	-3.367	0.038	Arachidonate 15-lipoxygenase	Down
TC520240	-1.61	0.047	n.i.	Down
ENSSSCT00000013027	-2.617	0.013	n.i.	Down
AK233548	-1.097	0.015	n.i.	Down
ENSSSCT00000011046	-1.297	0.015	n.i.	Down
AK230687	-2.509	0.015	n.i.	Down
ENSSSCT00000011934	-1.895	0.016	n.i.	Down
A_72_P409998	0.929	0.007	n.i.	Up
TC601625	1.154	0.013	n.i.	Up
TC591961	0.592	0.015	n.i.	Up
TC540937	2.522	0.015	n.i.	Up
TC526711	3.032	0.029	n.i.	Up
AK232497	2.857	0.04	n.i.	Up
Combined treated areas FDR between 5% and 10%				
NM_214037	-1.42	0.093	Ameloblastin	Down
DQ845172	-1.5	0.097	Beta-2-microglobulin	Down
NM_213990	-1.51	0.093	C-type lectin domain family 5, member A	Down
NM_213776	-1.26	0.093	CD2 molecule	Down
NM_214155	-1.18	0.093	CD247 molecule	Down
NM_001008691	-3.35	0.093	Chemokine (C-X-C motif) ligand 10	Down
NM_001114289	-3.97	0.097	Chemokine (C-X-C motif) ligand 9	Down
NM_001003924	-1.89	0.093	Complement component 1, q subcomponent, A-chain	Down
NM_214153	-1.32	0.093	Ectonucleoside triphosphate diphosphohydrolase 1	Down
NM_214000	-0.95	0.008	Haptoglobin	Down
NM_213813	-2.46	0.063	Killer cell lectin-like receptor subfamily K, member 1	Down
NM_001097415	-0.81	0.089	Lymphocyte antigen 86	Down
NM_001113706	-1.64	0.093	MHC class II DR-alpha	Down
NM_213811	-2.36	0.076	Scavenger receptor for phosphatidylserine and oxidized low density lipoprotein	Down
ENSSSCT00000007803	-1.72	0.081	Similar to cystatin F	Down
AK232017	-2.63	0.097	Similar to signaling threshold-regulating transmembrane adapter 1 precursor (suppression-inducing transmembrane adapter 1) (SHP2-interacting transmembrane adapter protein) (gp30/40)	Down
NM_001001632	-1.45	0.08	Tropomyosin 3	Down
NM_213883	3.05	0.063	Insulin-like growth factor 2 (somatomedin A)	Up
NM_001134346	1.41	0.093	Kruppel-like factor 11	Up
NM_001025222	1.39	0.097	Myozenin 1	Up
ENSSSCT00000007708	0.92	0.093	Prion protein	Up
ENSSSCT00000011141	1.01	0.093	Similar to glyceronephosphate O-acyltransferase	Up
AY609888	0.67	0.081	Similar to NAD(P) dependent steroid dehydrogenase-like	Up
AY609888	0.78	0.097	Similar to NAD(P) dependent steroid dehydrogenase-like	Up

Further not identified genes at FDR 5-10%: downregulated: EW261758, NM_001243319, AK397775, DN121339, TC533994, TC544302, L21161, ENSSSCT00000000690, NM_001161643, ENSSSCT00000005170, A_72_P418159, A_72_P418159, AK394244, TC594134, TC569821, CK451290, TC608152, AK230519, TC591665, TC544851, NM_001256770, TC555560, ENSSSCT00000017072, A_72_P773461, TC611786, AK239173; and **upregulated in APOSEC-treated animals:** TC543654, TC614889, BX923234, AK349090.

FDR: false discovery rate, n.i.: not identified genes.

infarction showed trend towards higher expression in APOSEC-treated animals. MEF2c expression was induced and showed significant overexpression in the gene array when FDR <20% was used.

4.3. Limitations

Control animals received local intramyocardial injections of medium solution, therefore the gene expression might be different from that in non-treated infarcted animals. Therefore it is not appropriate to conduct a direct comparison of our “medium-solution-treated” control group with literature data that describe gene patterns in rodent ischemic/reperfusion hearts [30] or in rodent or pig chronic ischemia/infarction models using placebo, sham operation or no treatment in control animals [25–28,31].

Macroscopic identification of the real border zone of the infarction at day 60 that corresponds to the injected area at day 30 is crucial for obtaining valuable information from the experiments. In this study, localizing the LAD segment close to the origin of the second diagonal branch where the occlusion was made previously and identifying the margin of the infarcted area proved technically feasible. In addition, the differences in the gene expression profiles in the normal, border, and infarct areas confirmed that these areas were sampled correctly.

5. Conclusions

APOSEC attenuates chronic myocardial ischemia-induced ventricular remodeling in a clinically relevant large animal model. Specifically, APOSEC induced long-lasting differences in gene expression that led to silencing of genes involved in apoptosis and inflammation. The gene profiling results identified genes that represent targets for anti-remodeling and anti-ischemic therapy.

Conflict of interest

The authors declare competing financial interests. The Medical University of Vienna has a claimed financial interest (patent number EP2201954, WO2010070105-A1, filed 18 Dec 2008). HJA is a shareholder of Aposcience AG, which owns the rights to commercialize APOSEC for therapeutic use.

Funding

This study was funded by the Christian Doppler Research Association (Vienna, Austria), Aposcience AG (Vienna, Austria), the Ludwig Boltzmann Institute, and the Medical University of Vienna.

Appendix A. Supplementary data

Supplementary data related to this article can be found at <http://dx.doi.org/10.1016/j.biomaterials.2013.12.071>.

References

- [1] Orlic D, Kajstura J, Chimenti S, Limana F, Jakoniuk I, Quaini F, et al. Mobilized bone marrow cell repair the infarcted heart, improving function and survival. *Proc Natl Acad Sci USA* 2001;98:10344–9.
- [2] Jeevanantham V, Butler M, Saad A, Abdel-Latif A, Zuba-Surma EK, Dawn B. Adult bone marrow cell therapy improves survival and induces long-term improvement in cardiac parameters: a systematic review and meta-analysis. *Circulation* 2012;126:551–6.
- [3] Martín-Rendon E, Brunskill S, Dorée C, Hyde C, Watt S, Mathur A, et al. Stem cell treatment for acute myocardial infarction. *Cochrane Database Syst Rev* 2008;(4):CD006536.
- [4] Thum T, Bauersachs J, Poole-Wilson PA, Volk HD, Anker SD. The dying stem cell hypothesis: immune modulation as a novel mechanism for progenitor cell therapy in cardiac muscle. *J Am Coll Cardiol* 2005;46:1799–802.
- [5] Saas P, Bonnefoy F, Kury-Paulin S, Kleinclauss F, Perrche S. Mediators involved in the immunomodulatory effects of apoptotic cells. *Transplantation* 2007;84(Suppl. 1):31–4.
- [6] Gnechi M, Zang Z, Ni A, Dzau VJ. Paracrine mechanisms in adult stem cell signaling and therapy. *Circ Res* 2008;103:1204–19.
- [7] Korf-Klingebiel M, Kempf T, Sauer T, Brinkmann E, Fischer P, Meyer GP, et al. Bone marrow cells are a rich source of growth factors and cytokines: implications for cell therapy trials after myocardial infarction. *Eur Heart J* 2008;29:2851–8.
- [8] Di Santo S, Yang Z, Wyler von Ballmoos M, Voelzmann J, Diehm N, Baumgartner I, et al. Novel cell free strategy for therapeutic angiogenesis: in vitro generated conditioned medium can replace progenitor cell transplantation. *PLoS One* 2009;4:e5643.
- [9] Lichtenauer M, Mildner M, Baumgartner A, Hasun M, Werba G, Beer L, et al. Intravenous and intramyocardial injection of apoptotic white blood cell suspensions prevents ventricular remodeling by increasing elastin expression in cardiac scar tissue after myocardial infarction. *Basic Res Cardiol* 2011;106:645–55.
- [10] Ankersmit HJ, Hoetzenecker K, Dietl W, Soleiman A, Horvat R, Wolfsberger M, et al. Irradiated cultured apoptotic peripheral blood mononuclear cells regenerate infarcted myocardium. *Eur J Clin Invest* 2009;39:445–56.
- [11] Lichtenauer M, Mildner M, Hoetzenecker K, Zimmermann M, Podesser BK, Sipos W, et al. Secretome of apoptotic peripheral blood cells (APOSEC) confers cytoprotection to cardiomyocytes and inhibits tissue remodelling after acute myocardial infarction: a preclinical study. *Basic Res Cardiol* 2011;106:1283–97.
- [12] Hoetzenecker K, Zimmermann M, Hoetzenecker W, Schweiger T, Kollmann D, Mildner M, et al. Mononuclear cell secretome protects from experimental autoimmune myocarditis. *Eur Heart J* 2013 Jan 14. <http://dx.doi.org/10.1093/eurheartj/ehs459>.
- [13] Freyman T, Polin G, Osman H, Crary J, Lu M, Cheng L, et al. A quantitative, randomized study evaluating three methods of mesenchymal stem cell delivery following myocardial infarction. *Eur Heart J* 2006;27:1114–22.
- [14] Dixon JA, Gorman RC, Stroud RE, Bouges S, Hirotsugu H, Gorman 3rd JH, et al. Mesenchymal cell transplantation and myocardial remodelling following myocardial infarction. *Circulation* 2009;120(Suppl. 11):S220–9.
- [15] Cheng Y, Yi G, Conditt GB, Sheehy A, Kolodgie FD, Tellez A, et al. Catheter based endomyocardial delivery of mesenchymal precursor cells using 3D echo guidance improves cardiac function in a chronic myocardial injury ovine model. *Cell Transplant* 2013;22:2299–309.
- [16] Xiang F, Shi Z, Guo X, Qiu Z, Chen X, Huang F, et al. Proteomic analysis of myocardial tissue from the border zone during early stage post-infarct remodelling in rats. *Eur J Heart Fail* 2011;13:254–63.
- [17] Yndestad A, Neurauder CG, Oie E, Forström RJ, Vinge LE, Eide L, et al. Up-regulation of myocardial DNA base excision repair activities in experimental heart failure. *Mutat Res* 2009;666:32–8.
- [18] Gyöngyösi M, Dib N. Diagnostic and prognostic value of 3D NOGA mapping in ischemic heart disease. *Nat Rev Cardiol* 2011;8:393–404.
- [19] Heiberg E, Sjögren J, Ugander M, Carlsson M, Engblom H, Arheden H. Design and validation of segment – a freely available software for cardiovascular image analysis. *BMC Med Imaging* 2010;10:1–13.
- [20] Core team. R: A language and environment for statistical computing. Vienna, Austria: R Foundation for Statistical Computing; 2012. <http://www.R-project.org/>.
- [21] Smyth GK. *limma: Linear Models for Microarray Data*. In: Gentleman R, Carey V, Huber W, Irizarry R, Dudoit S, editors. *Bioinformatics and computational biology solutions using R and bioconductor*. New York: Springer; 2005. pp. 397–420.
- [22] Huang da W, Sherman BT, Lempicki RA. Systematic and integrative analysis of large gene lists using DAVID bioinformatics resources. *Nat Protoc* 2009;4:44–57.
- [23] Ranganath SH, Levy O, Inamdar MS, Karp JM. Harnessing the mesenchymal stem cell secretome for the treatment of cardiovascular disease. *Cell Stem Cell* 2012;10:244–58.
- [24] Ertel A, Tozeren A. Human and mouse switch-like genes share common transcriptional regulatory mechanisms for bimodality. *BMC Genomics* 2008;9:628.
- [25] Jin H, Yang R, Awad TA, Wang F, Li W, Williams SP, et al. Effects of early angiotensin-converting enzyme inhibition on cardiac gene expression after acute myocardial infarction. *Circulation* 2001;103:736–42.
- [26] Sehl PD, Tai JT, Hillan KJ, Brown LA, Goddard A, Yang R, et al. Application of cDNA microarrays in determining molecular phenotype in cardiac growth, development, and response to injury. *Circulation* 2000;101:1990–9.
- [27] Stanton LW, Garrard LJ, Damm D, Garrick BL, Lam A, Kapoun AM, et al. Altered patterns of gene expression in response to myocardial infarction. *Circ Res* 2000;86:939–45.
- [28] Song GY, Wu YJ, Yang YJ, Li JJ, Zhang HL, Pei HJ, et al. The accelerated post-infarction progression of cardiac remodelling is associated with genetic changes in an untreated streptozotocin-induced diabetic rat model. *Eur J Heart Fail* 2009;11:911–21.
- [29] Prat-Vidal C, Gálvez-Montón C, Nonell L, Puigdecant E, Astier L, Solé F, et al. Identification of temporal and region-specific myocardial gene expression patterns in response to infarction in swine. *PLoS One* 2013;8:e54785.
- [30] Roy S, Khanna S, Kuhn DE, Rink C, Williams WT, Zweier JL, et al. Transcriptome analysis of the ischemia-reperfused remodeling myocardium: temporal changes in inflammation and extracellular matrix. *Physiol Genomics* 2006;25:364–74.
- [31] Jameel MN, Li Q, Mansoor A, Qiang X, Sarver A, Wang X, et al. Long-term functional improvement and gene expression changes after bone marrow-derived multipotent progenitor cell transplantation in myocardial infarction. *Am J Physiol Heart Circ Physiol* 2010;298:H1348–56.